Surface precision of optical membranes with curvature

D. K. Marker

Advanced Optics and Imaging Division, Air Force Research Laboratory
3550 Aberdeen Ave SE
Kirtland AFB, NM 87117-5776

markerd@plk.af.mil

C. H. Jenkins

Mechanical Engineering Dept. SD School of Mines and Technology, Rapid City, SD 57701

Abstract: Space-based inflatable technology is of current interest to NASA and DOD, and in particular to the Air Force and Phillips Laboratory. Potentially large gains in lowering launch costs, through reductions in structure mass and volume, are driving this activity. Diverse groups are researching and developing this technology for radio and radar antennae, optical telescopes, and solar power and propulsion applications. Regardless of the use, one common requirement for successful application is the accuracy of the inflated surface shape. The work reported here concerns the shape control of an inflated thin circular disk through use of a nonlinear finite element analysis. First, a review of the important associated Hencky problem is given. Then we discuss a shape modification, achieved through enforced boundary displacements, which resulted in moving the inflated shape towards a desired parabolic profile. Minimization of the figure error is discussed and conclusions are drawn.

OCIS codes: (230.4040) Mirrors; (310-0310) Thin films

References and links

1. Jenkins, C.H., and Leonard, J.W., "Nonlinear Dynamic Response of Membranes: State of the Art," *Appl. Mech. Rev. 44, 319-328* (1991).
2. Jenkins, C.H., "Nonlinear Dynamic Response of Membranes: State of the Art – Update," *Appl. Mech. Rev. 49 (10), S41-*S48 (1996).
3. Hencky, H., "Uber den Spannungszustand in kreisrunden Platten," *Z. Math. Phys*. 63, 311-317 (1915).
4. Föppl, A., "Vorlesungen uber technische Mechanik," *B.G. Teubner*, Bd. 5., p. 132, Leipzig, Germany (1907).
5. von Kármán, T., "Festigkeitsproblem im Naschinenbau," *Encyk. D. Math. Wiss.* **IV**, 311-385 (1910).
6. Stevens, H.H., "Behavior of circular membranes stretched above the elastic limit by air pressure," *Exp. Stress Anal*. 2, 139-146 (1944).
7. Chien, W.Z., "Asymptotic behavior of a thin clamped plate under uniform normal pressure at very large deflection," *Sci. Rep. Natn. Tsing Hua Univ.* A5, 71-94 (1948).
8. Kao, R., and Perrone, N., "Large deflections of axisymmetric circular membranes," *Int. J. Solids Struct.* **7**, 1601-1612 (1971).
9. Cambell, J.D., "On the theory of initially tensioned circular membranes subjected to uniform pressure," *Q. J. Mech. Appl. Math.* **9**, 84-93 (1956).
10. Dickey, R.W., "The plane circular elastic surface under normal pressure," *Arch. Ration. Mech. Anal.* **26**, 219-236 (1967).
11. Weil, N.A., and Newmark, N.M., " Large plastic deformations of circular membranes," *J. Appl. Mech.* **22**, 533-538 (1955).
12. Kao, R., and Perrone, N., "Large deflections of flat arbitrary membranes," *Comput. Struct.* **2**, 535-546 (1972).

#2668- $10.00 US Received September 16, 1997; Revised October 1, 1997

13. Shaw, F.S., and Perrone, N., "A numerical solution for the non-linear deflection of membranes," *J. Appl. Mech.* **21**, 117-128 (1954).
14. Schmidt, R., and DaDeppo, D.A., "A new approach to the analysis of shells, plates, and membranes with finite deflections," *Int. J. Non-Linear Mech.* **9**, 409-419 (1974).
15. Schmidt, R., "On Berger's method in the non-linear theory of plates," *J. Appl. Mech.* **41**, 521-523 (1974).
16. Storakers, B., "Small deflections of linear elastic circular membranes under lateral pressure," *J. Appl. Mech.* **50**, 735-739 (1983).
17. Weinitschke, H.J., "On axisymmetric deformations of nonlinear elastic membranes," *Mech. Today* **5**, 523-542, Pergamon Press, Oxford (1980).
18. Weinitschke, H.J., "On finite displacements of circular elastic membranes," *Math. Method Appl. Sci.* **9**, 76-98 (1987).
19. Weinitschke, H.J., "Stable and unstable axisymmetric solutions for membranes of revolution," *Appl. Mech. Rev.* **42**, S289-S294 (1989).
20. Ciarlet, P.G., "A justification of the von Kármán equations," *Arch. Ration. Mech. Anal.* **73**, 349-389 (1980).
21. Pujara, and Lardner, T.J., "Deformations of elastic membranes–effect of different constitutive relations," *Z. Angew. Math. Phys.* **29**, 315-327 (1978).
22. Thomas, M., and Veal, G. (1984), "Highly accurate inflatable reflectors," *AFRPL TR-84-021*.
23. Murphy, L.M., "Stretched-membrane heliostat technology," *J. Solar Energy Eng.* **108**, 230-238 (1986).
24. Murphy, L.M., "Moderate axisymmetric deformations of optical membrane surfaces," *J. Solar Energy Eng.* **109**, 111-120 (1987).
25. Palisoc, A., and Thomas, M., "A comparison of the performance of seamed and unseamed inflatable concentrators," *Solar Engineering 1995, Proc. 1995 ASME/JSME/JSES Int. Solar Energy Conf.*, **2**, 855-864 (1995).
26. Basart, J. P., Mandayam, S.A., and Burns, J.O., "An inflatable antenna for space-based low-frequency radio astronomy," *Proc. Space '94: Engineering, Construction, and Operations in Space IV* - Vol. 2, Albuquerque, NM (1994).
27. Cassapakis, C., and Thomas, M., "Inflatable structures technology development overview," *AIAA* 95-3738 (1995).
28. Chow, P.Y., "Construction of pressurized, self-supporting membrane structure on the moon," *J. Aerospace Eng.* **5**, 274-281 (1992).
29. Grossman, G., and Williams, G., "Inflatable concentrators for solar propulsion and dynamic space power," *J. Solar Energy Eng.* **112**, 229-236 (1990).
30. Malone, P.K., and Williams, G.T., "A lightweight inflatable solar array," *Proc. 9th Annual AIAA/USU Conference on Small Satellites*, Logan, UT (1995).
31. Nowak, P.S., Sadeh, W.Z., and Janakus, J., "Feasibility study of inflatable structures for lunar base," *J. Spacecraft Rockets* **31**, 453-457 (1994).
32. Rogers, C.A., Stultzman, W.L., Campbell, T.G., and Hedgepeth, J.M., "Technology assessment and development of large deployment antennas," *J. Aerospace Engineering* **6**(1), 34-54 (1993).
33. Sadeh, W.Z., and Criswell, M.E., "A generic inflatable structure for a lunar/Martian base," *Space IV, Proc. Space '94*, Albuquerque, ASCE, 1146-1156 (1994).
34. Hedgepeth, J.M., "Accuracy potentials for large space antenna reflectors with passive structures," *J. Spacecraft* **19**(3), 211-217 (1982).
35. Vaughn, H., "Pressurizing a prestretched membrane to form a paraboloid," *Int. J. Eng. Sci.* **18**, 99-107 (1980).
36. Hart-Smith, L.J., and Crisp, J.D.C., "Large elastic deformations of thin rubber membranes," *Int. J. Eng. Sci.* **5,** 1-24 (1967).
37. Natori, M., Shibayama, Y., and Sekine, K., "Active accuracy adjustment of reflectors through the change of element boundary," AIAA 89-1332 (1989).
38. Jenkins, C.H., Marker, D.K., and Wilkes, J.M., "Improved surface accuracy of precision membrane reflectors through adaptive rim control," *AIAA Adaptive Structures Forum*, Long Beach, CA (to appear) (1998a).
39. Jenkins, C.H., Wilkes, J.M., and Marker, D.K., "Surface accuracy of precision membrane reflectors," *Space 98*, Albuquerque, NM (to appear) (1998b).

After a brief history in space over four decades ago, a resurgence of interest in membrane structures for extraterrestrial use is developing. Applications for such structures range from planar configurations in solar sails, concentrators, and shields, to inflatable lenticulars for radar, radio, and optical uses.

Three key factors are paramount for the success and user acceptance of this technology: deployment, longevity, and performance. Performance hinges critically on the precision of the membrane surface. The amount of precision is highly mission dependent, and may entail one or more of the following issues: surface smoothness, deviation from desired surface profile, and slope error. Parabolic profiles are most commonly desired. The most prominent systemic error found in circular inflated or vacuumed membranes is a spherical aberration. This aberration is often

#2668- $10.00 US Received September 16, 1997; Revised October 1, 1997

referred to as a "W-profile error," which is a measure of the deviation of the actual surface from that of the desired configuration.

For example, the AF Phillips Laboratory has recently undertaken the task of creating a large optical quality membrane telescope. The membranes on these telescopes will range in thickness from 10 - 150 micrometers. The maximum acceptable peak-to-peak figure error over the entire surface will range from 10 - 20 micrometers. (This value assumes that a certain amount of adaptive optics will be used to correct image errors.). This paper will discuss a particular means for reducing the figure error.

We begin by first reviewing the problem of the inflation of an initially plane, circular membrane, with deformations limited to those that admit only small strains but moderately large rotations. (We purposefully exclude here any consideration of the associated problems of the inflation of annular membranes or circular plates, or of large strain deformation. [1],[2]) Next we discuss the particular requirements of a precision membrane reflector. Then we use finite element analysis to demonstrate the effects of boundary (rim) control on the deformed shape of an inflated circular membrane. Finally we discuss results and draw conclusions.

Review of the Hencky problem is in order. Consider the geometry of Figure 1, which represents a plane elastic sheet, with circular boundary of radius a. The geometry is rotationally symmetric (axisymmetric); we also assume the loading to be a symmetric pressure p. The sheet has modulus E and Poisson's ratio n.

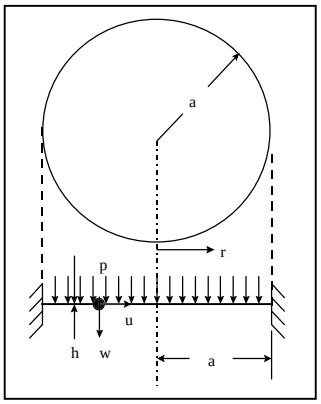

Fig. 1. Definition Sketch

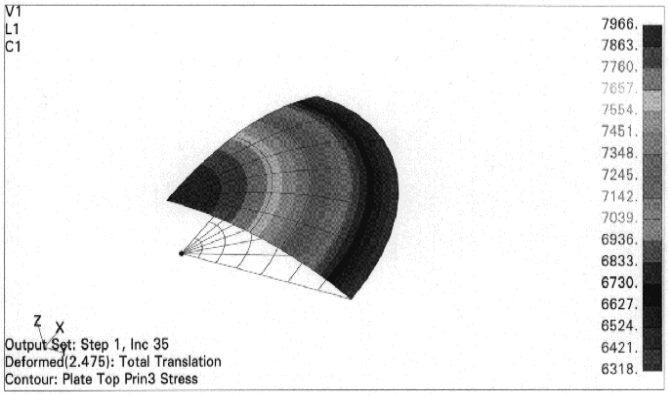

Fig.2. Inflated Membrane (3-D view)

The problem of the inflation of an initially plane membrane with circular boundary begins with Hencky. [3] Earlier, Föppl [4] had arrived at equilibrium equations for a membrane plate. These equations were essentially modified von Kármán plate equations [5] with the bending rigidity set to zero. The von Kármán plate equations are based upon strains which have nonlinearity introduced through rotations (squares of slope):

$$\varepsilon_r = \frac{du}{dr} + \frac{1}{2}\left(\frac{dw}{dr}\right)^2 \tag{1}$$

$$\varepsilon_\theta = \frac{u}{r} \tag{2}$$

where u and w are displacements in the r and z directions, respectively.

The von Kármán plate equations in axisymmetric form can be written as:

$$D\left(\frac{d^2}{dr^2} + \frac{1}{r}\right)^2 w - \frac{h}{r}\frac{d}{dr}\left(\frac{d\Phi}{dr}\frac{dw}{dr}\right) = p \tag{3}$$

#2668- $10.00 US Received September 16, 1997; Revised October 1, 1997

$$r\frac{d}{dr}\left(\frac{d^2\Phi}{dr^2}+\frac{1}{r}\frac{d\Phi}{dr}\right)+\frac{E}{2}\left(\frac{dw}{dr}\right)^2=0 \tag{4}$$

where $D = Eh^3/12(1-\nu^2)$ is the bending rigidity, and ϕ is a stress function to which the stress resultants in the radial and circumferential direction are related respectively by:

$$\sigma_r=\frac{1}{r}\frac{d\Phi}{dr},\sigma_\theta=\frac{d^2\Phi}{dr^2} \tag{5}$$

Linear elastic constitutive relations are assumed. It is important to note that the above equations are not *geometrically exact*, in that small angle assumptions have been made.

Hencky provided a solution of the above for the case of zero boundary displacements (u = 0 = w at r = a) and D = 0 by assuming power series for stresses and transverse displacement. Little interest in the Hencky problem seems to have taken place until the 1940's, when, in conjunction with a study on air-supported roofs, Stevens [6] performed an experimental investigation on a 10 inch radius by 0.014 inch thick cellulose acetate butyrate inflated circular membrane. Steven's compared his results for the deflected membrane shape (which were apparently empirical in nature) with Hencky's. Apparently Chien [7] provided slight corrections to Hencky's solutions for maximum values of stress and transverse deflection. [8]

Cambell [9] allowed an arbitrary initial tension in the membrane. Dickey [10] re-examined the Hencky problem, this time using a nonlinear integral equation formulation. Dickey provided a plot of u(r) for various values of the Poisson's ratio. Weil and Newmark [11] provide some experimental evidence that validate Dickey's predictions. We discuss later the important relationship of u(r) with the surface precision.

Kao and Perrone [12] used a relaxation method, developed earlier by Shaw and Perrone [13], to solve the Hencky problem. [12] Schmidt and DaDeppo [14] and Schmidt [15] used a perturbation analysis based on odd powers of r (actually r/a), in conjunction with the Marguerre shallow shell equations (which collapse to the von Kármán plate equations when there exists no initial curvature), to determine the maximum values of the stress and transverse displacement in the Hencky problem. In a series of articles, Storakers [16] uses a power series in even powers of r (or r/a) for stresses and transverse displacement (odd powers of r for u(r)).

Validity of the Föppl-von Kármán formulation for certain regimes of deformation is discussed by Weinitschke. [17] For the case of the axisymmetric deformation of an annular membrane, Weinitschke considered a parameter K, (essentially the so-called nondimensional load parameter), where

$$k=\left(\frac{2r_a p}{Eh}\right)^{\frac{1}{3}} \tag{6}$$

and r_a is the radius of the outer edge of the membrane. Comparisons were made between the Föppl and the large rotation Reissner shell (with zero bending stiffness) theories. For values of K > ½, the difference between theories exceeds 10%. The appropriateness of a Reissner-like theory for K > ½ is reiterated in Weinitschke [18]. [See also Storakers [16]; for further details on the Reissner theory see Weinitschke [19]; see also Ciarlet [20] for further justification of the von Kármán equations.] Pujara and Lardner [21] showed that linear (Hookean) and nonlinear (Mooney-Rivlin) elastic constitutive relations provide essentially similar Hencky results up to w_0/a equal to about 0.3.

Thomas and Veal [22] report on the surface precision measurements of membrane reflector, with various gore seaming configurations. They suggest that an rms surface error of 1 mm is suitable for membrane reflectors with frequency applications less than 15 Ghz. Plotting the deviation of the actual membrane surface from that of a true parabola results in a "W-shaped

#2668- $10.00 US Received September 16, 1997; Revised October 1, 1997

curve" or simply a "W-curve." Murphy [23],[24] studied "stretched membrane heliostats" (large, nearly flat, concentrating solar reflectors) which are inflated into a doubly-curved surface with f/D around 14. The surface profile was assumed to be parabolic, and initial tension was considered. An extension of Storakers [16] method was used to predict deformations up to w_0/a of about 0.035 (f/D = 3.6). Deviations from the perfect parabola were small, as would be expected for K on the order of 0.1. Palisoc and Thomas [25] suggest that the variation of elastic modulus with strain over the membrane surface can be large, and may be a major cause of surface inaccuracies.

There currently exists renewed interest in applications of precision inflatable structures in space. With increased pressure to reduce costs associated with design, fabrication, and launch of space structures, DOD and NASA are taking a new look at space-based inflatable structures. Applications for inflatable structures in space include lunar and planetary habitat, RF reflectors and waveguides, optical and IR imaging, solar concentrators for solar power and propulsion, sun shades, and solar sails. [26],[27],[28],[29],[30],[31],[32],[33]

For many of these applications, particularly those involved with communications, imaging, power, and propulsion, accurate maintenance of the inflatable surface shape is critical. Surface accuracy requirements are wavelength dependent. Optics generally require a tenth of a wavelength or better to be considered adequate. [34] The likelihood of achieving this range of accuracy by purely passive means is low.

It can be shown that the Hencky membrane never inflates identically to a parabola, absent other effects. Studies on varying the thickness distribution of the undeformed membrane to achieve either a parabolic [35] or spherical [36] profile upon inflation have shown that, in both of these cases, thickness must initially increase from center to edge in order to achieve either of these desired shapes. Natori et al. [37] showed that improvements toward the parabolic shape could be made by moving the boundary of initially curved beam strips. Our results presented below show that boundary manipulation can have beneficial impact on reducing the figure error in nonlinear membrane deformations. [38],[39]

In the FEM analysis that follows, we show that reductions in deviations of the inflated surface profile, from that of a desired parabola, can be achieved through boundary displacements. This is a precursor to more detailed studies on active profile control. ABAQUS was used for the FEM computation, while FEMAP was used for pre- and post-processing.

A quarter-symmetry model was used that consisted of 42 second-order shell elements (see comments below) and 177 nodes. (Note that for axisymmetric loading, only a "strip" of the disk needs to be modeled; however, for the boundary perturbation that follows, quarter-symmetry was required.) Figure 2 shows typical FEM results for the Hencky problem. Contours shown are for the radial stress component.

For the values of the parameters chosen here, viz., radius a = 21 in (53.3 cm), h = 0.005 in (0.13 mm), E = 500,000 psi (3.45 Mpa), and n = 0.4, and the bending rigidity D is extremely small (0.0062 lb×in), the disk is essentially a membrane. This can be demonstrated by comparing the deformed profiles using both pinned and clamped boundary conditions. There is no discernible difference between the two cases, since the bending rigidity is of insufficient value to enforce the zero-slope (clamped) boundary condition. Hence in what follows, we use shell finite elements, since these provide us with a richer array of choices in ABAQUS; pinned boundary conditions are used.

When analyzing this class of structures it is convenient to take as the solution to (3) and (4) the three-term polynomial

$$w = w_0\left(1+\alpha_2\frac{r^2}{a^2}+\alpha_4\frac{r^4}{a^4}\right) \tag{7}$$

#2668- $10.00 US Received September 16, 1997; Revised October 1, 1997

where w_0 is the deflection at r = 0, and a_2 and a_4 are constants which satisfy the boundary conditions. Using the membrane assumption and $\nu = 0.4$, the central deflection w_0 can be shown to be [Hencky, 1915]:

$$w_0 = 0.626a\left(\frac{pa}{Eh}\right)^{\frac{1}{3}} \tag{8}$$

In the present case, the boundary conditions (at r = a) are given by the displacement w = 0, and either one of the following two equivalent conditions:

$$M_r = D\left(\frac{d^2w}{dr^2} + \frac{\nu}{r}\frac{dw}{dr}\right) \tag{9}$$

or

$$\varepsilon_\theta = 0 \Rightarrow \sigma_\theta - \nu\sigma_r = 0 \Rightarrow \frac{d^2\Phi}{dr^2} - \frac{\nu}{r}\frac{d\Phi}{dr} \tag{10}$$

Note that (9) implies $D \neq 0$.

Taking the assumed deflected shape (7) and substituting into the above boundary conditions leads to the following expressions for the αs:

$$\alpha_2 = -\frac{6+2\nu}{5+\nu} \tag{11}$$

$$\alpha_4 = \frac{1+\nu}{5+\nu} \tag{12}$$

Note that (11) and (12) imply that the deflected shape is a function of w_0, r, and the Poisson's ratio only. For the Poisson's ratio of 0.4, the deflected shape becomes

$$w_b = w_0\left(1 - 1.259\frac{r^2}{a^2} + 0.245\frac{r^4}{a^4}\right) \tag{13}$$

The corresponding Hencky solution would reveal:

$$w_m = w_0\left(1 - 0.899\frac{r^2}{a^2} - 0.101\frac{r^4}{a^4}\right) \tag{14}$$

The equivalent parabola would be given by:

$$w_p = w_0\left(1 - \frac{r^2}{a^2}\right) \tag{15}$$

Figure 4 shows the displacement u(r); note the asymmetry in the distribution.

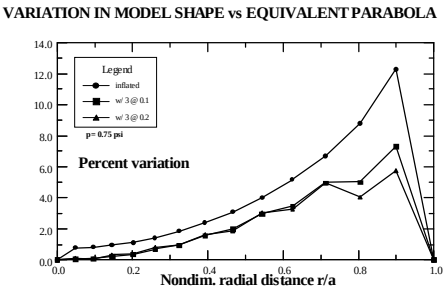

Fig. 3. Comparison Measurements Fig.

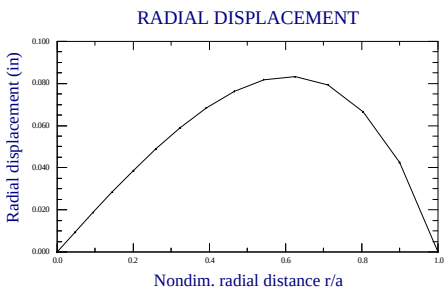

4. Radial Displacements

#2668- $10.00 US
Received September 16, 1997; Revised October 1, 1997

Boundary perturbations via radial displacements are now imposed on the FEM model after the inflation step. These displacements occur at the 0, 45, and/or 90 degree positions around the model boundary. The FEM model was perturbed with a 0.1 in (2.54 mm) outward radial displacements at each of the three angular positions. Note in figure 5 that the center deflection has decreased, and the radial stress has generally increased everywhere (disregarding the local stress concentrations at the displacement points). The model was utilized to predict the resulting shape with a 0.1 in radial outward displacements at the 0 and 90 degree positions.

We review the results while looking along the 45 degree meridian, regardless of whether a displacement is applied at the corresponding boundary point or not. The deflected profile (at the 45 degree meridian) was compared for three cases: (i) inflation only without boundary displacements, (ii) boundary displacements at the 0, 45, and 90 degree positions, and (iii) boundary displacements at the 0 and 90 degree positions. The reduction in overall deflection is evident. (Note that for convenience, each profile is forced through the same position r = a. There is a small and insignificant error introduced here, since the imposed boundary displacement is much smaller than the radius itself.)

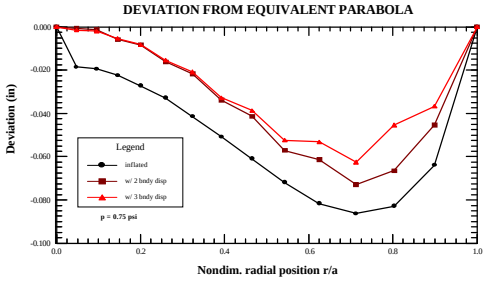

Fig. 5. Model Vs Parabola

Returning now to the "W" problem discussed above, Figure 5 shows the effect of boundary displacement on reducing the W-curve, where all data is taken along the 45 degree meridian. The 3 boundary displacements case shows the maximum reduction in the W-curve (displacement directly at 45 degree meridian); however, even with only 2 displacements (0 and 90 degrees), the W-error is reduced along the 45 degree meridian.

In conclusion the inflated membrane reflectors are formed from initial plane sheets, clamped in circular boundaries, and deformed into curved surfaces. It has been demonstrated that these surfaces are not true paraboloids. However, the deviation of the membrane profile from parabolic may be reduced by appropriate displacements at the boundary. From the examples shown above, the maximum deviation ranges from about 12.5% for the inflated only case, to a little over 7% for 3 boundary displacements, a 58% reduction. These results lay grounds for future investigations leading toward active control of reflector surfaces.

APPENDIX

It was shown that the coefficients in the equation for the surface profile w(r/a) are functions of Poisson's ratio. We note also that the membrane stiffness, k_m

$$k_m = \frac{Eh}{1-\nu^2} \tag{1a}$$

depends as well on Poisson's ratio, as it should. That is, for all real multi-dimensional deformations, material displaced in one direction always occurs at the expense of material displaced in (arbitrarily) transverse directions.

#2668- $10.00 US
Received September 16, 1997; Revised October 1, 1997

Consider a thin rectangular strip of width "a" and length "b". The edges "a" are clamped, and a uniform tensile force is applied normal to these edges. For any boundary conditions on edges "b", material extension in the force direction comes at the expense of a contraction in the transverse directions; this is directly related to the physical meaning of the Poisson's ratio. Now consider the following two cases: 1) edges "b" remain free; 2) edges "b" are constrained not to displace transverse to the force direction (but are free to extend in the force direction. Since, for the same applied force, it is more difficult to transversely contract material in case 2 (where it is "transversely held") than for case 1, the extension in the force direction is less for case 2 than for case 1, and case 2 *appears* stiffer than case 1. *A priori*, this *apparent* stiffening might be attributed to an *apparent* Poisson's ratio in case 2 which was different (less) than that in case 1.

(The stiffening effect of boundary conditions is easily demonstrated in the simpler case of beam deformation. Comparing the transverse deflection under the same transverse force for identical pinned-pinned or clamped-clamped beams, the clamped-clamped beam deflects less and *appears*, and *is*, stiffer than the pinned-pinned case.)

Now returning to the membrane stiffness k_m above, it is verified that as Poisson's ratio decreases, the membrane stiffness increases. Let us know consider an initially circular plane membrane, deformed under pressure loading, made of material with *variable* Poisson's ratio. (A variable Poisson's ratio is not without precedent in membrane mechanics: see Stein and Hedgepeth, 1961; Mikulas, 1964; Miller et al., 1985.)

At the fixed boundary (r = a), by definition $\varepsilon_\theta = 0$, and

$$\varepsilon_\theta = 0 \Rightarrow \sigma_\theta = \nu\sigma_r \tag{2a}$$

Or, cast in terms of an *apparent* Poisson's ratio,

$$\nu(r=a) = \frac{\sigma_\theta}{\sigma_r} \tag{3a}$$

It can be readily shown that at r = a, $\sigma_\theta < \sigma_r$ [e.g., see Stevens, 1944], and hence the apparent Poisson's ratio here is less than one.

As the apex (r = 0) of the membrane is approached from r = a, (in deference to the singularity in the circumferential strain at r = 0), the circumferential strains (stresses) approach the radial strains (stresses) in value, and the *apparent* Poisson's ratio approaches unity.

We now form the ratio of membrane stiffness as

$$\frac{k_m(r=0)}{k_m(r=a)} = \frac{1-\left[\nu(a)\right]^2}{1-\left[\nu(0)\right]^2} > 1 \tag{4a}$$

That is, the membrane is locally stiffer at the apex than at the boundary. Since the displacement depends on the stiffness, the membrane stretches (hence deflects) proportionately more at the edge than at the center. This is the reason for the asymmetry in u(r) where, as seen in Figure 9, u(r) is greater toward the boundary than toward the apex (u(r) is maximum at about 0.62 r/a).

The above argument explains physically why the uniform membrane never inflates identically to a parabola, and why boundary displacements *radially outward* move the figure towards parabolic.

#2668- $10.00 US Received September 16, 1997; Revised October 1, 1997